

Real-space renormalization-group approach to the multigrid method

Vikram Vyas*

Physics Department, Boston University, Boston, Massachusetts 02215

(Received 27 November 1989; revised manuscript received 20 September 1990)

We establish the connection between the multigrid algorithms and the real-space renormalization group. This is illustrated with the example of the two-dimensional Euclidean Klein-Gordon equation with random mass. The equation is then numerically solved using a two-level multigrid algorithm.

I. INTRODUCTION

Simulation of lattice gauge theories¹⁻⁴ with fermionic degrees of freedom requires repeated inversion of the Dirac operator in the presence of a prescribed gauge field.⁵ Such an operator is represented on the lattice by a large, sparse matrix with fluctuating coefficients. The usual numerical methods employed for inverting sparse matrices involve some form of iterative scheme, and all such algorithms show a poor rate of convergence when applied to a Dirac operator with a realistic (small) quark mass. We shall refer to this as the problem of critical slowing down.⁶

Similar problems appear in the numerical analysis of partial differential equations (PDE's) and in this context the "multigrid" (MG) method was developed.^{7,8} It alleviates and in some cases eliminates the problem of critical slowing down. Since the Dirac equation is a PDE, it is natural to try and see whether the MG method would work for the Dirac equation.⁹ On the other hand, there are several features which distinguish the problem of calculating fermionic propagators from that of solving ordinary PDE's. Some of these are the presence of gauge fields and the fact that one has to average the fermionic propagator (or products of fermionic propagators) over quantum fluctuations of gauge fields. In fact, the direct application of MG methods faces problems in the presence of nonzero topological charge.¹⁰

In Ref. 9 (see also Ref. 11) it was suggested that one possible way of taking into account these features is to combine traditional multigrid methods with renormalization-group techniques in a gauge-invariant manner. In this paper we investigate this suggestion in the simpler context of inverting the Euclidean Klein-Gordon equation with a fluctuating mass in two dimensions. The important feature this model shares with the problem of calculating fermionic propagators is that both involve inverting a matrix with fluctuating coefficients.

In Sec. II we give a brief introduction to the MG approach. As described in Sec. II, the MG method involves solving for the smooth eigenmodes of the original operator on the coarse lattice. In Sec. III we address the question of what should be the form of the operator on the coarse lattice. In Secs. IV and V we use a real-space renormalization-group (RG) transformation to obtain one

possible form for this operator. In Sec. VI we present our numerical results. We state our conclusions in the final section. In Appendix A the connection between the RG approach to the MG method and the traditional approach⁸ is established.

II. MULTIGRID

Consider the linear equation

$$Lu = b. \quad (2.1)$$

L is a symmetric positive-definite linear operator defined on the lattice, and b is an external source; L will in general depend on some external field. Let us apply the simplest form of relaxation method, the Gauss-Jacobi algorithm, to solve Eq. (2.1). Although the algorithm is not the most efficient, we use it because it illustrates in a very clear manner the role played by the small eigenvalues in a relaxation algorithm.⁶

$$u^{(n+1)} = (1 - \epsilon L)u^{(n)} + \epsilon b, \quad (2.2)$$

where ϵ is the step size. The n th iterate can be written as

$$u^{(n+1)} = u^{(\infty)} - (1 - \epsilon L)^n \epsilon_0, \quad (2.3)$$

where e_0 is the initial error, defined as

$$e_0 = L^{-1}b - u^{(0)}.$$

For the iteration scheme to converge, $\|1 - \epsilon L\| < 1$, which can be ensured by choosing

$$\epsilon \approx \frac{1}{\lambda^+}, \quad (2.4)$$

where λ^+ is the largest eigenvalue of L . The component of error along the λ th eigenmode of L will evolve as

$$e_\lambda^{(n)} = (1 - \epsilon\lambda)^n e_\lambda^{(0)}, \quad (2.5a)$$

$$e_\lambda^{(n)} = \left[1 - \frac{\lambda}{\lambda^+}\right]^n e_\lambda^{(0)}, \quad (2.5b)$$

$$e_\lambda^{(n)} \approx \exp\left[-n \frac{\lambda}{\lambda^+}\right] e_\lambda^{(0)}. \quad (2.5c)$$

It follows from Eq. (2.5) that the number of iterations required to solve Eq. (2.1) is of order of

$$\tau = \frac{\lambda^+}{\lambda^-}, \quad (2.6)$$

where λ^- is the lowest eigenvalue of the operator L . τ , the relaxation time, tends to infinity as λ^- becomes small: This is the problem of critical slowing down.⁶

The central philosophy of the MG approach is that slow components of the error, components associated with low eigenvalues, can be well represented by a coarser lattice. Therefore, by projecting the error vector to a coarse lattice, we reduce the size of the problem while retaining the information about the relevant modes.⁷ We shall illustrate the idea with a two-grid algorithm. Start with a trial solution $u^{(0)}$ and iterate this solution ν times. Calculate the residue defined as

$$r^{(\nu)} = b - Lu^{(\nu)}. \quad (2.7)$$

Then the error

$$e^{(\nu)} = u^{(\infty)} - u^{(\nu)} \quad (2.8)$$

satisfies the equation

$$Le^{(\nu)} = r^{(\nu)}. \quad (2.9)$$

Solving Eq. (2.9) is equivalent to solving (2.1) as

$$u^{(\infty)} = u^{(\nu)} + e^{(\nu)}. \quad (2.10)$$

The MG approach is to solve Eq. (2.9) on a coarse lattice (in what follows we will assume that the coarse lattice constant is twice that of the original lattice). Denoting the quantities on the coarse lattice with a caret,

$$\hat{L}\hat{e}^{(\nu)} = \hat{r}^{(\nu)}, \quad (2.11)$$

where

$$\hat{r}^{(\nu)} = Pr^{(\nu)}, \quad (2.12)$$

and P is the operator which projects the residue vector r to the coarse lattice. \hat{L} is the coarse-grid version of the original operator L . We will consider one possible form for it in the next section. \hat{L} is smaller by a factor of 2^D than L , where D = number of dimensions. After having solved Eq. (2.11) on the coarse grid to some approximation, one interpolates the solution \hat{e} to the original lattice,

$$\bar{e} = I\hat{e}. \quad (2.13)$$

The interpolated value of the error vector is used in Eq. (2.10) to obtain a better approximation to the correct solution. This is called the coarse-grid correction and is given by

$$\bar{u}^{(\nu)} = u^{(\nu)} + \bar{e}. \quad (2.14)$$

To take into account the error introduced because of projection and interpolation, ν more iterations are done on the fine grid. This constitutes one cycle of a two-level MG algorithm. To solve Eq. (2.11) efficiently, one may again use a coarse-grid correction by introducing a new grid, with twice the lattice spacing of the coarse grid, thus defining a recursive algorithm.

III. FORM OF \hat{L}

We are interested in solving the linear equation

$$L\{\sigma\}\phi = b, \quad (3.1)$$

where $L\{\sigma\}$ is an operator defined on the fine lattice, which depends on the "external" field σ , and b is a source for the ϕ field. In the context of lattice gauge theory, ϕ is the analog of a matter field and σ that of a gauge field. In the multigrid algorithms we need to choose a coarse-grid operator \hat{L} which mimics the behavior of $L\{\sigma\}$ when acting on slowly varying fields. Going from a fine lattice to a coarse lattice corresponds to reducing degrees of freedom. The consequence of such a reduction can be followed using RG methods.¹²⁻¹⁴ RG transformations can be applied directly to Eq. (3.1), but from the point of view of lattice gauge theories, it is more convenient and natural to implement it on the action from which Eq. (3.1) can be derived. In Appendix A we show the equivalence of the two approaches.

Consider a field theory defined on the lattice by the action

$$S = S[\phi, \sigma] + S_g[\sigma], \quad (3.2)$$

$$S[\phi, \sigma] = \frac{1}{2}(\phi, L\{\sigma\}\phi). \quad (3.3)$$

$S_g[\sigma]$ is the part of the action which only depends on the σ field. To define this theory on the coarse lattice, we divide the fields into two parts:

$$\phi = \begin{bmatrix} \hat{\phi} \\ \tilde{\phi} \end{bmatrix}, \quad (3.4)$$

$$\sigma = \begin{bmatrix} \hat{\sigma} \\ \tilde{\sigma} \end{bmatrix},$$

where $\hat{\phi}$ and $\hat{\sigma}$ are the coarse degrees of freedom, while $\tilde{\phi}, \tilde{\sigma}$ are the degrees of freedom not present on the coarse grid. The action (3.2) is now reexpressed in terms of these new variables:

$$S\{\phi, \sigma\} = S\{\hat{\phi}, \hat{\sigma}, \tilde{\phi}, \tilde{\sigma}\}. \quad (3.5)$$

The next step is to integrate out the $\tilde{\phi}$ variables (see Appendix A) to obtain an effective action for the $\hat{\phi}$ variables on the coarse lattice:

$$\exp(-\hat{S}\{\hat{\phi}, \hat{\sigma}, \tilde{\sigma}\}) = \int D\tilde{\phi} \exp(-S\{\hat{\phi}, \hat{\sigma}, \tilde{\phi}, \tilde{\sigma}\}). \quad (3.6)$$

Then the action for the $\hat{\phi}$ variables can be written as

$$\hat{S}\{\hat{\phi}, \hat{\sigma}, \tilde{\sigma}\} = \frac{1}{2}(\hat{\phi}, \hat{L}\{\hat{\sigma}, \tilde{\sigma}\}\hat{\phi}). \quad (3.7)$$

Equation (3.7) defines one possible choice of the coarse-grid operator for a given σ -field configuration.

The operator defined by means of Eq. (3.7) depends on both the $\hat{\sigma}$ and the $\tilde{\sigma}$ variables. If the coarse-grid variables are obtained by blocking of the fine variables, as is the case in our model problem (see Sec. V), then the $\hat{\sigma}$ variables contain the information about the long-wavelength modes of the original σ configuration and the $\tilde{\sigma}$ variables have the information about the short-wavelength modes.¹² This motivates us to explore the

possibility of approximating $\hat{L}\{\hat{\sigma},\bar{\sigma}\}$ by an operator which is only a function of the $\hat{\sigma}$ variables. It is also possible that eliminating the dependence over the $\bar{\sigma}$ variables is not the desirable thing to do in a given situation, and one should not reduce the degrees of freedom for the σ field and, therefore, obtain \hat{L} as a function of both the $\hat{\sigma}$ and the $\bar{\sigma}$ variables. This is indeed the case in the successful application of algebraic MG techniques to the random-resistor problem.¹⁵ We will study this issue in the context of our model both analytically in Sec. V and numerically in Sec. VI.

\hat{L} as defined by Eq. (3.7) is in general a nonlocal operator which is practically impossible to calculate. Fortunately, for MG we do not need the full form of \hat{L} , but only its action on the slow modes (see Sec. II). Therefore, for the MG algorithm we can replace \hat{L} by \hat{L}_{approx} as long as

$$(\Psi_{\text{slow}}, \hat{L} \Psi_{\text{slow}}) \approx (\Psi_{\text{slow}}, \hat{L}_{\text{approx}} \Psi_{\text{slow}}), \quad (3.8)$$

where Ψ_{slow} are the states spanned by the slow modes of \hat{L} . The simplest form of approximation which one can try is

$$\hat{L}_{\text{approx}} = L\{(2a), \hat{\lambda}, \hat{m}\}, \quad (3.9)$$

where a is the lattice constant of the fine lattice and $\hat{\lambda}$ and \hat{m} are the renormalized coupling constant and mass.⁹ In this approximation \hat{L}_{approx} has the same form as that of L , apart from renormalization of the parameters appearing in it. In the next two sections we will investigate the conditions under which such an approximation may be possible.

IV. EUCLIDEAN KLEIN-GORDON OPERATOR WITH VARIABLE MASS

One of the features, as noted in the Introduction, which distinguishes the Dirac operator on the lattice is that it is represented by a sparse matrix with fluctuating coefficients. To study the effect of such randomness in a simpler context, we consider the two-dimensional Euclidean Klein-Gordon operator with a position-dependent mass term. This leads us to consider the equation

$$-\sum_{\mu} (\phi_{x+\mu} + \phi_{x-\mu}) + (K + \lambda\sigma_x)\phi_x = b_x, \quad (4.1)$$

with

$$K = 4 + m^2 a^2, \quad (4.2)$$

$$\lambda = a^2 g, \quad (4.3)$$

$$b_x = a^2 J_x. \quad (4.4)$$

J_x is the external source for the ϕ field, a is the lattice constant, and m is the mass of the ϕ field. The effect of the σ field is to give a position-dependent mass term to the ϕ field; g measures the strength of coupling between the ϕ and σ fields. We would like to use a MG algorithm for inverting Eq. (4.1). The model can be described by the action

$$S = S_1 + S_2 + \sum_x \phi_x b_x, \quad (4.5)$$

$$S_1 = \frac{1}{2} \sum_{x,y} \left[-\phi_x \sum_{\mu} (\delta_{x+\mu,y} + \delta_{x-\mu,y} - 2\delta_{x,y}) \phi_y + \phi_x a^2 (m^2 \delta_{x,y} + g \sigma_x \delta_{x,y}) \phi_y \right], \quad (4.6)$$

$$S_2 = \frac{1}{2} \sum_{x,y} \left[-\sigma_x \sum_{\mu} (\delta_{x+\mu,y} + \delta_{x-\mu,y} - 2\delta_{x,y}) \sigma_y + a^2 \rho^2 \sigma_x \delta_{x,y} \sigma_y \right], \quad (4.7)$$

where ρ is the mass of the σ field. We will consider the case where the coarse lattice, to be used in the MG algorithm, is obtained by blocking the sites of the fine lattice, as in Fig. 1. Corresponding to this blocking of sites, we group the values of the fields into a four-component field. These four-component fields live on the sites of the coarse lattice:

$$\Phi_{\bar{x}} = \begin{bmatrix} \phi_{\bar{x}}^{(1)} \\ \phi_{\bar{x}}^{(2)} \\ \phi_{\bar{x}}^{(3)} \\ \phi_{\bar{x}}^{(4)} \end{bmatrix}, \quad (4.8)$$

where \bar{x} labels the sites of the coarse lattice. Similarly, we group the σ field in a four-component field Σ . Now we rewrite the action (4.5) in terms of the coarse-grid variables Φ and Σ ; this can be done in a convenient manner using the notations of Refs. 16 and 17:

$$S_1 = \frac{1}{2} \sum_{\bar{x}, \bar{y}} \left[\frac{\Phi_{\bar{x}}^T}{2} \sum_{\mu} (-T_{\mu}^{(+)} \partial_{\mu}^{(2)} + T_{\mu}^{(-)} \partial_{\mu}^{(c)}) \Phi_{\bar{y}} \right] + \frac{1}{2} \sum_{\bar{x}} \Phi_{\bar{x}}^T M \Phi_{\bar{x}} + \frac{1}{2} \lambda \sum_{\bar{x}} \Phi_{\bar{x}} \bar{\sigma} \Phi_{\bar{x}}, \quad (4.9)$$

$$S_2 = \frac{1}{2} \sum_{\bar{x}, \bar{y}} \left[\frac{\Sigma_{\bar{x}}^T}{2} \sum_{\mu} (-T_{\mu}^{(+)} \partial_{\mu}^{(2)} + T_{\mu}^{(-)} \partial_{\mu}^{(c)}) \Sigma_{\bar{y}} \right] + \frac{1}{2} \sum_{\bar{x}} \Sigma_{\bar{x}}^T N \Sigma_{\bar{x}}, \quad (4.10)$$

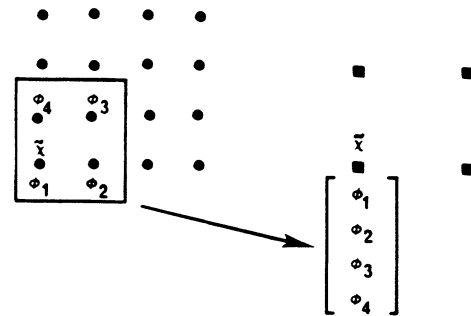


FIG. 1. Blocking of the sites to obtain the block lattice.

where the matrices T and $\bar{\sigma}$ are defined in Appendix B, and

$$\partial_{\mu}^{(2)} = \delta_{\bar{y}, \bar{x}+2\mu} + \delta_{\bar{y}, \bar{x}-2\mu} - 2\delta_{\bar{x}, \bar{y}}, \quad (4.11)$$

$$\partial_{\mu}^{(c)} = \delta_{\bar{y}, \bar{x}+2\mu} - \delta_{\bar{y}, \bar{x}-2\mu}. \quad (4.12)$$

M and N are the so-called mass matrices defined by

$$M = K - 2 \sum_{\mu} T_{\mu}^{+}, \quad (4.13)$$

$$N = H - 2 \sum_{\mu} T_{\mu}^{+}, \quad (4.14)$$

and $H = 4 + \rho^2 a^2$. In terms of the block fields, the partition function becomes

$$Z = Z_0 \int \prod_{\bar{x}} d\Phi_{\bar{x}} d\Sigma_{\bar{x}} \exp(-S\{\Phi, \Sigma\}). \quad (4.15)$$

At this stage we have reformulated the model onto a coarse lattice while keeping the same number of degrees of freedom as on the fine lattice.

V. BLOCK-SPIN TRANSFORMATION

In order to thin out the degrees of freedom, we separate the fields Φ and Σ into an average block field and fields which take into account fluctuations within a given block. First, consider the Φ field; the separation can be done by the following similarity transformation, implemented by the matrix R :

$$\xi_{\bar{x}} = R \Phi_{\bar{x}}, \quad (5.1)$$

$$\xi = \begin{bmatrix} \hat{\phi} \\ \tilde{\phi} \end{bmatrix}, \quad (5.2)$$

where

$$\hat{\phi} = \frac{1}{2}(\phi_1 + \phi_2 + \phi_3 + \phi_4), \quad (5.3)$$

$$\tilde{\phi} = \frac{1}{2} \begin{bmatrix} \phi_1 + \phi_2 - \phi_3 - \phi_4 \\ \phi_1 - \phi_2 - \phi_3 + \phi_4 \\ \phi_1 - \phi_2 + \phi_3 - \phi_4 \end{bmatrix} = \begin{bmatrix} \tilde{\phi}_1 \\ \tilde{\phi}_2 \\ \tilde{\phi}_3 \end{bmatrix}. \quad (5.4)$$

$\hat{\phi}$ is the block field apart from normalization, while $\tilde{\phi}$ represent the fluctuations. These fields are the analogs of $\hat{\phi}$ and $\tilde{\phi}$ of Sec. III. In order to obtain the equation of motion for $\hat{\phi}$, we must integrate out the fluctuations $\tilde{\phi}$ (see Appendix A). A similar separation can be done for the Σ field:

$$\eta = R \Sigma, \quad (5.5)$$

$$\eta = \begin{bmatrix} \hat{\sigma} \\ \tilde{\sigma} \end{bmatrix}. \quad (5.6)$$

We shall refer to the above transformation as a block-spin transformation^{16,17} (BST). Under the BST, the mass matrix (4.13), (4.14) becomes diagonal:

$$\tilde{M} = RMR^T, \quad (5.7)$$

$$\tilde{M} = \begin{bmatrix} m^2 a^2 & 0 & 0 & 0 \\ 0 & 4 + m^2 a^2 & 0 & 0 \\ 0 & 0 & 4 + m^2 a^2 & 0 \\ 0 & 0 & 0 & 8 + m^2 a^2 \end{bmatrix}. \quad (5.8)$$

The fluctuating fields are much heavier than the block field; in particular, $\tilde{\phi}_3$ is the heaviest mode. The action (4.1) can be reexpressed in terms of the block-spin-transformed fields. Explicit calculation shows that $\tilde{\phi}_3$ decouples from the block field $\hat{\phi}$, and in view of its large mass, we shall neglect it. With this approximation we have the following fields on the block lattice:

$$\xi = \begin{bmatrix} \hat{\phi} \\ \tilde{\phi} \end{bmatrix}, \quad (5.9)$$

$$\eta = \begin{bmatrix} \hat{\sigma} \\ \tilde{\sigma} \end{bmatrix}, \quad (5.10)$$

where now the fluctuating fields $\tilde{\phi}$ and $\tilde{\sigma}$ have only two components. These components correspond to fluctuations within a block along the two coordinate axes (see Fig. 2):

$$\tilde{\phi} = \begin{bmatrix} \tilde{\phi}_1 \\ \tilde{\phi}_2 \end{bmatrix}, \quad (5.11)$$

$$\tilde{\sigma} = \begin{bmatrix} \tilde{\sigma}_1 \\ \tilde{\sigma}_2 \end{bmatrix}. \quad (5.12)$$

The next step in integrating out the fluctuations is to go to momentum space on the block lattice, with lattice spacing $\hat{a} = 2a$. The range of momenta will then be

$$\frac{-\pi}{\hat{a}} < p_{\mu} \leq \frac{\pi}{\hat{a}} \quad (5.13)$$

and for convenience we shall define $\tilde{k}_{\mu} = p_{\mu} \hat{a}$. Let \tilde{n}^2 be the number of points on the block lattice. The block action can be rewritten as

$$S = S_a + S_b + S_c + S_d + S_e + S_f, \quad (5.14)$$

where

$$S_a = \frac{1}{2} \sum_{\bar{k}} \hat{\phi}^*(\bar{k}) \{ -[\cos(\tilde{k}_1) + \cos(\tilde{k}_2) - 2] + m^2 a^2 \} \hat{\phi}(\bar{k}) \\ + \frac{\lambda}{4\tilde{n}} \sum_{\bar{k}, \bar{l}} \hat{\phi}^*(\bar{k} + \bar{l}) \hat{\sigma}(\bar{l}) \hat{\phi}(\bar{k}), \quad (5.15)$$

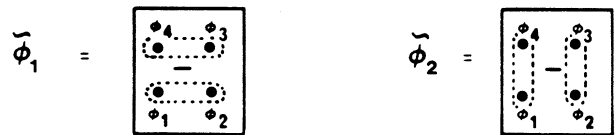


FIG. 2. Definition of the $\tilde{\phi}$ fields.

$$\begin{aligned}
S_b = & \frac{1}{2} \sum_{\vec{k}} \tilde{\phi}_1^*(\vec{k}) \{ -[\cos(\vec{k}_1) - \cos(\vec{k}_2)] + K \} \tilde{\phi}_1(\vec{k}) \\
& + \frac{\lambda}{4\tilde{n}} \sum_{\vec{k}, \vec{l}} \tilde{\phi}_1^*(\vec{k} + \vec{l}) \tilde{\sigma}(\vec{l}) \tilde{\phi}_1(\vec{k}) \\
& + \frac{1}{2} i \left[\sum_{\vec{k}} \tilde{\phi}_1^*(\vec{k}) \sin(\vec{k}_2) \hat{\phi}(\vec{k}) \right. \\
& \quad \left. - \sum_{\vec{k}} \hat{\phi}^*(\vec{k}) \sin(\vec{k}_2) \tilde{\phi}_1(\vec{k}) \right], \quad (5.16)
\end{aligned}$$

$$S_d = \frac{1}{2} \sum_{\vec{k}} \hat{\sigma}^*(\vec{k}) \{ -[\cos(\vec{k}_1) + \cos(\vec{k}_2) - 2] + \rho^2 a^2 \} \hat{\sigma}(\vec{k}), \quad (5.17)$$

and

$$\begin{aligned}
S_e = & \frac{1}{2} \sum_{\vec{k}} \tilde{\sigma}_1^*(\vec{k}) \{ -[\cos(\vec{k}_1) - \cos(\vec{k}_2)] + N \} \tilde{\sigma}_1(\vec{k}) \\
& + \frac{1}{2} i \sum_{\vec{k}} [\tilde{\sigma}_1^*(\vec{k}) \sin(\vec{k}_2) \hat{\sigma}(\vec{k}) - \hat{\sigma}^*(\vec{k}) \sin(\vec{k}_2) \tilde{\sigma}_1(\vec{k})] \\
& + \frac{\lambda}{4\tilde{n}} \sum_{\vec{k}, \vec{l}} [\tilde{\phi}_1^*(\vec{k} + \vec{l}) \tilde{\sigma}_1(\vec{l}) \hat{\phi}(\vec{k}) \\
& \quad + \hat{\phi}^*(\vec{k}) \tilde{\sigma}_1^*(\vec{l}) \tilde{\phi}_1(\vec{k} + \vec{l})]. \quad (5.18)
\end{aligned}$$

S_c and S_f are obtained from S_b and S_e , respectively, by interchanging subscripts 1 and 2. In terms of BST variables, the partition function has the form

$$Z = Z_0 \int \prod_x d\hat{\phi} d\hat{\sigma} d\tilde{\phi} d\tilde{\sigma} \exp(-S\{\hat{\phi}, \hat{\sigma}, \tilde{\phi}, \tilde{\sigma}\}). \quad (5.19)$$

Before integrating out the $\tilde{\phi}$ variables, let us rewrite Eqs. (5.14)–(5.18) in the symbolic but more transparent form

$$S = S[\hat{\phi}] + S[\tilde{\phi}] + S[\hat{\sigma}] + S[\tilde{\sigma}], \quad (5.20)$$

$$S[\hat{\phi}] = \frac{1}{2} \left[\hat{\phi}, \left[-\hat{\delta}^2 + m^2 a^2 + \frac{\lambda}{2} \hat{\sigma} \right] \hat{\phi} \right], \quad (5.21)$$

$$\begin{aligned}
S[\tilde{\phi}] = & \frac{1}{2} \left[\tilde{\phi}, \left[-\tilde{\delta}^2 + \left[K + \frac{\lambda}{2} \hat{\sigma} \right] \right] \tilde{\phi} \right] \\
& + (\tilde{\phi}, \partial^c \hat{\phi}) + \frac{\lambda}{4} (\tilde{\phi}, \tilde{\sigma} \hat{\phi}), \quad (5.22)
\end{aligned}$$

$$S[\hat{\sigma}] = \frac{1}{2} (\hat{\sigma}, (-\hat{\delta}^2 + \rho^2) \hat{\sigma}), \quad (5.23)$$

$$S[\tilde{\sigma}] = \frac{1}{2} (\tilde{\sigma}, (-\tilde{\delta}^2 + H) \tilde{\sigma}) + (\tilde{\sigma}, \partial^c \hat{\sigma}), \quad (5.24)$$

where $-\hat{\delta}^2$ and $-\tilde{\delta}^2$ represent the kinetic energy terms for the caretted and the tilded variables, ∂^c is the central derivative on the lattice, and K and H are defined via Eqs. (4.2) and (4.14), respectively. The integration over the $\tilde{\phi}$ variables can be done exactly but formally; as for an arbitrary σ field configuration, the quadratic form in the integrand is not positive definite. We will continue with this formal analysis as finally we will resort to a perturbative calculation for \hat{L} , which is valid for small values of λ . The result of the integration is

$$\begin{aligned}
S_{\text{eff}}[\hat{\phi}, \sigma, \tilde{\sigma}] = & S[\hat{\phi}] - \frac{1}{2} \left(\partial^c \hat{\phi}, A^{-1} \{ \hat{\sigma} \} \partial^c \hat{\phi} \right) \\
& + \frac{\lambda}{2} (\partial^c \hat{\phi}, A^{-1} \{ \hat{\sigma} \} \tilde{\sigma} \hat{\phi}) \\
& + \frac{\lambda^2}{16} (\tilde{\sigma} \hat{\phi}, A^{-1} \{ \hat{\sigma} \} \tilde{\sigma} \hat{\phi}) \Big], \quad (5.25a)
\end{aligned}$$

$$= (\hat{\phi}, \hat{L} \{ \hat{\sigma}, \tilde{\sigma} \} \hat{\phi}). \quad (5.25b)$$

$A^{-1} \{ \hat{\sigma} \}$ is the propagator for the $\tilde{\phi}$ field in the presence of the fixed $\hat{\sigma}$ field (see Fig. 3). In obtaining Eq. (5.25) we have neglected $\det[A^{-1} \{ \hat{\sigma} \}]$ as it does not effect the equation of motion for the $\hat{\phi}$ field. \hat{L} defined by Eq. (5.25) is a nonlocal operator and does not have the same form as L [Eq. (4.1)]. This form of \hat{L} , as it stands, is of little value for the implementation of a MG algorithm. Hence let us investigate the conditions under which one can simplify (5.25).

The $\tilde{\sigma}$ field enters in the effective action through the last two terms in Eq. (5.25). Consider the last but one term: This term is of the order of

$$\lambda A^{-1} \{ \hat{\sigma} \} \approx \frac{\lambda}{K} \approx \frac{\lambda}{4}, \quad (5.26)$$

which is small even in the case when $\lambda \approx m^2 a^2$. Similarly, the last term in Eq. (5.25) is of the order of $\lambda^2/4$. The reason that the effects of these terms are relatively small can be traced to the fact that we could implement a blocking scheme on the ϕ and σ fields in which the fields, $\tilde{\phi}$ and $\tilde{\sigma}$, representing fluctuations within the block, have a very large mass on the scale of the inverse lattice spac-

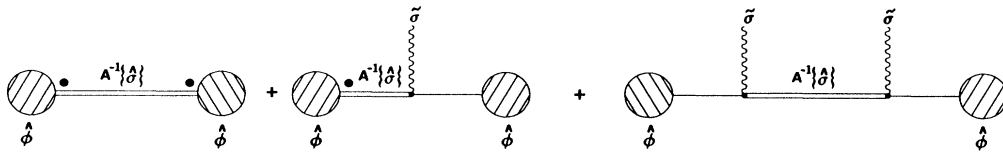


FIG. 3. Result of integrating the $\tilde{\phi}$ variables (● above a line represents the derivative of the adjacent field).

ing [see Eqs. (5.1)–(5.8)]. In view of the relative smallness of these terms, we will neglect them. It is in this approximation that we obtain \hat{L} which is a function of the $\hat{\sigma}$ variables alone. Let us now consider the effect of the second term in Eq. (5.25). In the leading perturbative approximation for $A^{-1}\{\hat{\sigma}\}$, this term combines with $S[\hat{\phi}]$ to give, in the long-wavelength limit,

$$S_{\text{eff}}^0[\hat{\phi}] = \frac{1}{2} \sum_{\vec{k}} \hat{\phi}^*(\vec{k}) [(\vec{k}_1^2 + \vec{k}_2^2) + \hat{m}^2 \hat{a}^2] \hat{\phi}(\vec{k}) + \hat{\lambda}/2\bar{n} \sum_{\vec{k}, \vec{l}} \hat{\phi}^*(\vec{k} + \vec{l}) \hat{\sigma}(\vec{l}) \hat{\phi}(\vec{k}), \quad (5.27)$$

with $\hat{a} = 2a$ and $\hat{\lambda} = \hat{a}^2 g$. This is the same as the original action, in the long-wavelength limit, on the fine lattice, except for a rescaling of the lattice constant. The $\hat{\phi}$ and $\hat{\sigma}$ fields are now normalized so that they correspond to the block-average fields. We will use \hat{L} defined via Eq. (5.27) in a numerical study of a two-level MG algorithm. One of the aims of our numerical experiments will be to check the validity of the approximations made in obtaining Eq. (5.27).

VI. NUMERICAL STUDY OF TWO-DIMENSIONAL EUCLIDEAN KLEIN-GORDON EQUATION WITH RANDOM MASS

As a first step in determining the effectiveness of MG algorithms, we consider the equation

$$-\left[\sum_{\mu=1}^2 (\phi_{x+\mu} + \phi_{x-\mu}) \right] + [4 + a^2(m^2 + g\sigma_x)] \phi_x = a^2 b_x, \quad (6.1)$$

where a is the lattice constant, m is the mass of the ϕ field, and b is an external source. σ_x is a random external field, which takes values from a Gaussian distribution:

$$P[\sigma_x] = \frac{1}{(\sqrt{2\pi})} \exp(-\frac{1}{2}\sigma_x^2). \quad (6.2)$$

Because of the random field, the effective mass varies around m^2 with a root-mean-square deviation equal to g . The model differs from the model considered in Secs. IV and V in that the action for the σ field is

$$S\{\sigma\} = \frac{1}{2} \sum_x \sigma_x^2, \quad (6.3)$$

and the randomness is “quenched” rather than “annealed.”

Using the analysis of Sec. V, we consider the following form for \hat{L} :

$$(\hat{L}\hat{\phi})_{\vec{x}} = - \sum_{\vec{\mu}=1}^2 (\hat{\phi}_{\vec{x}+\vec{\mu}} + \hat{\phi}_{\vec{x}-\vec{\mu}}) + [4 + \hat{a}^2(m^2 + g\hat{\sigma}_{\vec{x}})] \hat{\phi}_{\vec{x}}, \quad (6.4)$$

where

$$\hat{a} = 2a. \quad (6.5)$$

This is precisely the Galerkin choice⁸ of the coarse-grid

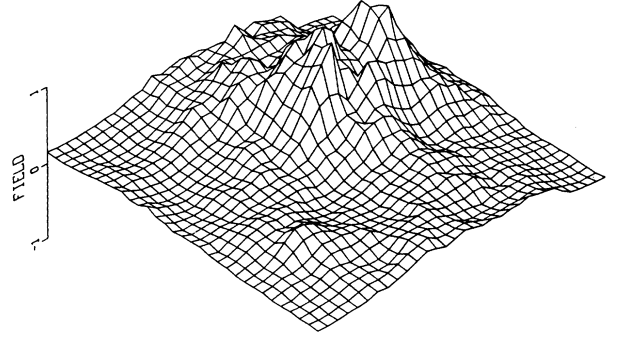


FIG. 4. Lowest eigenfunction of L .

operator corresponding to piecewise constant interpolation.

We used the simplest form of relaxation algorithm, the Gauss-Jacobi method, to invert Eq. (6.1) with periodic boundary conditions. As remarked in Sec. II, the Gauss-Jacobi method is not the most efficient algorithm for inverting Eq. (6.1), but it has the virtue of showing in a clear manner the effects of the lowest eigenmodes of the operator on the relaxation process. The lowest eigenfunction of L for a lattice of size 32^2 with $g=0.25$ is shown in Fig. 4; it shows a marked degree of localization. This is not surprising, since Eq. (6.1) with (6.2) is similar to the Anderson model which exhibits localization.¹⁸

We studied the problem of inverting Eq. (6.1) on lattices of size 64^2 , 128^2 , and 256^2 with and without the two-level MG algorithm. We implemented the two-level MG by first applying $\nu_1=4$ iterations of the Gauss-Jacobi algorithm on the fine lattice. Then we go down to a coarse lattice obtained by blocking the fine lattice and solve for the error equation [see Eq. (2.11)] by applying $\nu_2=4$ iterations of the Gauss-Jacobi algorithm. Finally, we come back to the fine grid and apply ν_1 more itera-

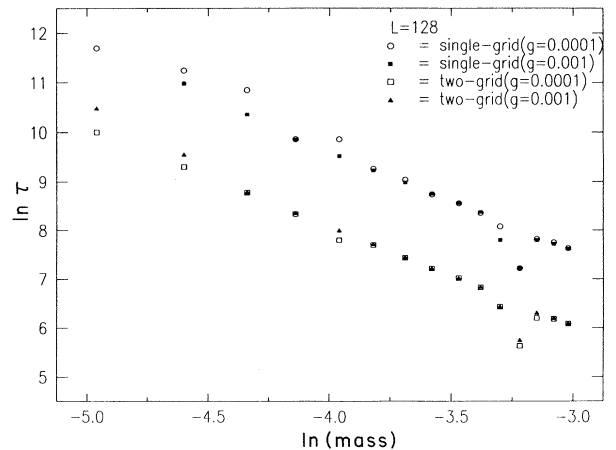


FIG. 5. $\ln(\tau)$ vs $\ln(\text{mass})$ for $L = 128$.

TABLE I. Results for $L = 64$.

Mass	g	$\frac{g}{m^2}$	$L = 64$			No. conf.
			τ_{sg}	τ_{mg}	eff	
0.01	0.0001	1.0	50 329	10 849	4.63	25
0.02	0.0004	1.0	12 641	2 691	4.70	50
0.03	0.0009	1.0	5 786	1 203	4.80	50
0.02	0.0012	3.0	12 696	2 707	4.69	50
0.02	0.0024	6.0	12 388	2 787	4.44	50
0.02	0.0036	9.0	13 561	2 946	4.60	50

tions. This cycle was repeated until the norm of the residue was less than 0.005.

One of the motivation in doing these numerical experiments was to see the effect of randomness on the performance of the MG algorithm. This was done by evaluating the performance of the MG algorithm for various values of g/m^2 and m , over a number of distinct configurations of the σ field. Our results are presented in Tables I–III, where we define the efficiency (eff) as the ratio of the average value of τ [see Eqs. (2.5c) and (2.6)] for a single grid to τ for the two-level MG algorithm. In each case we see that the two-level MG algorithm decreases the average relaxation time by a factor of at least 4, but as expected, this does not eliminate the critical slowing down (see Fig. 5; [the dip in Fig. 5 occurs for the value of m for which the algorithm on the top grid becomes optimum for the fixed chosen value of the step size ϵ of Eq. (2.2)]) as it is still, with two levels, a local algorithm. The efficiency of the algorithm showed large fluctuations for a small-sized lattice, $L = 64^2$ (see Fig. 6), but decreased for the larger lattice $L = 256^2$ (see Fig. 7) with the value of g/m^2 kept constant. In all the cases studied, we find that the efficiency of the algorithm remained fairly constant for a wide range of randomness, as measured by the value of g/m^2 . This is consistent with the fact

that the RG corrections to \hat{L} are in each of these cases small, being of the order of $g/4$ (see Sec. V).

The main result of our preliminary investigations is that the MG algorithms are effective even for operators with fluctuating coefficients, in the range suggested by RG analysis.

VII. CONCLUSIONS

In this article we have established a connection between the real-space RG method and the multigrid algorithms. RG provides us with one possible form of the coarse-grid operator \hat{L} , which has the desired property of reproducing the correct infrared physics on the coarse lattice. This is of utmost importance for MG algorithms as we want to solve for the long-wavelength modes of the original operator on the coarse lattice. In the traditional approach to MG, one chooses a simple form for \hat{L} , which is usually obtained from the original operator L by replacing the lattice constant a by $2a$. From the computational point of view, such a form of \hat{L} is desirable, and therefore we would like to know if the traditional approach would work in a given situation. This can be answered by an approximate RG calculation of \hat{L} , thus determining the range of conditions under which the

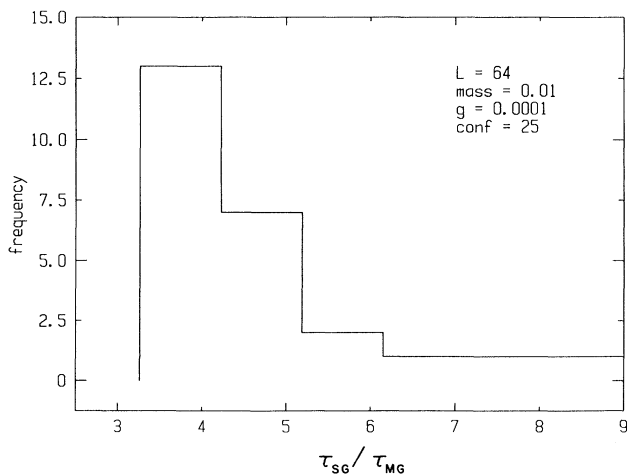


FIG. 6. Fluctuations in the efficiency of the two-level MG algorithm for $L = 64$.

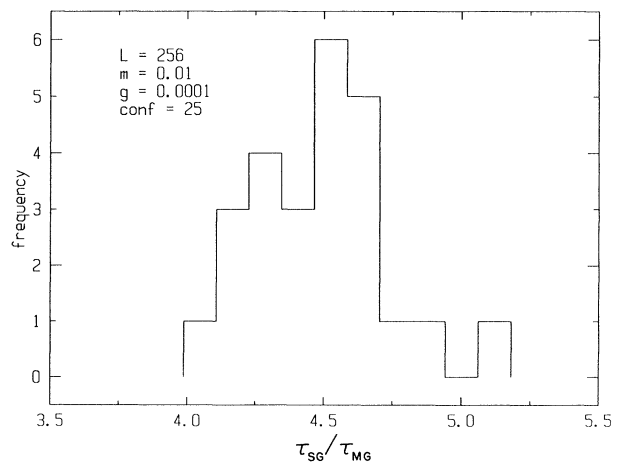


FIG. 7. Fluctuations in the efficiency of the two-level MG algorithm for $L = 256$.

TABLE II. Results for $L = 256$.

Mass	g	$\frac{g}{m^2}$	$L = 256$			No. conf.
			τ_{sg}	τ_{mg}	eff	
0.01	0.0001	1.0	48 244	10 780	4.48	25
0.02	0.0004	1.0	5507	1142	4.82	25
0.03	0.0009	1.0	5574	1185	4.70	25
0.03	0.003	3.3	5582	1193	4.68	25
0.03	0.006	6.7	5725	1226	4.67	25
0.03	0.009	10.0	6017	1286	4.68	25

traditional MG algorithms will be effective. Outside this range an approximate RG analysis indicates that the form of \hat{L} has to be modified. Such a modification usually involves introducing next-nearest-neighbor interactions and renormalizing the parameters appearing in the original operator L . We have extended this analysis to the case of fermionic propagators in lattice gauge theories.¹⁹ This was done by obtaining \hat{L} in the Migdal-Kadanoff approximation.²⁰ The numerical properties of this operator are currently under investigation.

ACKNOWLEDGMENTS

It is a pleasure to thank Professor C. Rebbi for suggesting this problem, and for many helpful discussions and constant encouragement. I am grateful to Professor R. C. Brower for several useful conversations. I would also like to thank Sona Prakash for carefully reading the manuscript and for various useful suggestions. Support from the U.S. Department of Energy (Contract No. DE-AC02-89ER40509) is also gratefully acknowledged.

TABLE III. Results for $L = 128$.

Mass	g	$\frac{g}{m^2}$	$L = 128$			No. conf.
			τ_{sg}	τ_{mg}	eff	
0.007	0.0001	2.04	119 912	22 180	5.4	50
0.010	0.0001	1.0	76 440	10 932	7.0	50
0.013	0.0001	0.59	51 355	6 482	7.9	50
0.016	0.0001	0.39	19 067	4 201	4.5	50
0.019	0.0001	0.28	19 123	2 974	6.4	50
0.022	0.0001	0.21	10 460	2 217	4.7	50
0.025	0.0001	0.16	8 458	1 711	4.9	50
0.028	0.0001	0.13	6 244	1 368	4.6	50
0.031	0.0001	0.10	5 220	1 116	4.7	50
0.034	0.0001	0.09	4 291	924	4.6	50
0.037	0.0001	0.07	3 239	620	5.2	50
0.040	0.0001	0.06	1 370	279	4.9	50
0.043	0.0001	0.05	2 497	491	5.0	50
0.046	0.0001	0.05	2 314	481	4.8	50
0.049	0.0001	0.04	2 053	437	4.7	50
0.007	0.001	20.4		35 786		23
0.010	0.001	10.0	58 885	14 075	4.5	50
0.013	0.001	5.9	31 720	6 600	4.8	50
0.016	0.001	3.9	18 965	4 270	4.4	50
0.019	0.001	2.8	13 659	2 992	4.6	50
0.022	0.001	2.1	10 214	2 246	4.5	50
0.025	0.001	1.6	7 942	1 717	4.6	50
0.028	0.001	1.3	6 383	1 370	4.7	50
0.031	0.001	1.0	5 286	1 124	4.7	50
0.034	0.001	0.9	4 358	931	4.7	50
0.037	0.001	0.7	2 437	623	3.9	50
0.040	0.001	0.6	1 371	315	4.4	50
0.043	0.001	0.5	2 436	551	4.4	50
0.046	0.001	0.5	2 257	495	4.6	50
0.049	0.001	0.4	2 038	442	4.6	50

APPENDIX A

In this appendix we will establish the connection between the coarse-grid operator defined by means of the RG transformation (see Sec. III) and the coarse-grid operator defined via so-called Galerkin condition.⁸

Consider the following linear equation defined on the fine grid:

$$L\phi = b, \quad (\text{A1})$$

where L is a symmetric positive-definite operator. We wish to find its form on the coarse grid. Let us assume that there exists an interpolation operator I such that

$$\phi \approx I\hat{\phi}, \quad (\text{A2})$$

where $\hat{\phi}$ is the field defined on the coarse grid. Equation (A2) is statement of the assumed smoothness of the slow modes (see Sec. II). Using Eq. (A2) in (A1), we obtain

$$LI\hat{\phi} = b. \quad (\text{A3})$$

Applying the projection operator P [defined by Eq. (2.12)] to both sides of Eq. (A3) leads to

$$PLI\hat{\phi} = \hat{b}. \quad (\text{A4})$$

From Eq. (A4) we obtain the Galerkin condition for the coarse-grid operator:

$$\hat{L} = PLI. \quad (\text{A5})$$

In order to make the connection between Eq. (A5) and the \hat{L} defined in Sec. III, consider the case when the coarse grid is obtained by decimation²⁰ (generalization to the case of blocking will become apparent.) Let the coarse grid be defined by the “even” sites $\phi_e = \hat{\phi}$, while the fine grid is defined by both the “even” and the “odd” sites ϕ_o . Equation (A1) can be rewritten in the symbolic form

$$\begin{pmatrix} L_{oo} & L_{oe} \\ L_{oe} & L_{ee} \end{pmatrix} \begin{pmatrix} \phi_o \\ \phi_e \end{pmatrix} = \begin{pmatrix} b_o \\ b_e \end{pmatrix}. \quad (\text{A6})$$

The next step in the RG approach is to solve for the ϕ_o in terms of the ϕ_e ; this can be done algebraically or in terms of the “functional” integral. Let us first solve for the ϕ_o algebraically. A simple calculation leads to following equation for the ϕ_e variables alone:

$$(L_{ee} - L_{oe}L_{oo}^{-1}L_{oe})\phi_e = (b_e - L_{oe}L_{oo}^{-1}b_o). \quad (\text{A7})$$

Equation (A7) provides us with the explicit form for the \hat{L} and the projection operator P :

$$\hat{L} = L_{ee} - L_{oe}L_{oo}^{-1}L_{oe}, \quad (\text{A8})$$

$$\hat{b} = Pb, \quad (\text{A9})$$

$$P = (-L_{oe}L_{oo}^{-1}). \quad (\text{A10})$$

Let us now consider the form of the interpolation operator I . In order to interpolate $\hat{\phi}$ to ϕ , we will solve for the ϕ_o in terms of the ϕ_e with the b_o set to zero (as there are no “odd” points on the coarse grid) and thus obtaining

$$\phi_o = -L_{oo}^{-1}L_{oe}\phi_e. \quad (\text{A11})$$

This allows us to define I as

$$I = \begin{pmatrix} -L_{oo}^{-1}L_{oe} \\ 1 \end{pmatrix} = P^T. \quad (\text{A12})$$

Instead of solving for the ϕ_o in terms of the ϕ_e algebraically, one could consider the Gaussian integral

$$Z = \int D\phi \exp[-\frac{1}{2}(\phi, L\phi) + (b, \phi)], \quad (\text{A13})$$

where the integrand is the “action” corresponding to Eq. (A1). Again, separating the degrees of freedom into the “odd” ϕ_o and the “even” ϕ_e , we obtain

$$Z = \int D\phi_e D\phi_o \exp[-\frac{1}{2}(\phi_e, L_{ee}\phi_e) + (b_e, \phi_e) - \frac{1}{2}(\phi_o, L_{oo}\phi_o) + (b_o - \phi_e L_{oe}, \phi_o)]. \quad (\text{A14})$$

Solving for ϕ_o is equivalent to integrating over them in Eq. (A14). The result of this integration is

$$Z = \text{const} \times \int D\phi_e \exp[-\frac{1}{2}(\phi_e, \hat{L}\phi_e) + (\hat{b}, \phi_e)], \quad (\text{A15})$$

where the \hat{L} and the \hat{b} are same as those given by Eqs. (A8) and (A9).

Coming back to the Galerkin condition (A5), it is easy to see that the \hat{L} given by Eq. (A8) satisfies (A5) with the projection and interpolation operators given by Eqs. (A10) and (A12), respectively. Condition (A5) in itself does not tell us the explicit form of the projection and interpolation operators, while the RG approach provides us with one possible form. The advantage of this, as noted in Sec. III, is that by construction \hat{L} will reproduce the infrared physics of the L on the coarse grid.¹² Unfortunately, \hat{L} given by Eq. (A8) can be calculated exactly only for the one-dimensional cases.¹⁹ For more realistic cases we need an approximate way of implementing the RG prescription. Such an approximation, whether perturbative as in Sec. V or nonperturbative as the Migdal-Kadanoff approximation,²⁰ is most conveniently expressed in the language of functional integrals.

APPENDIX B

The explicit form of T matrices is

$$T_1^+ = \begin{pmatrix} 0 & 1 & 0 & 0 \\ 1 & 0 & 0 & 0 \\ 0 & 0 & 0 & 1 \\ 0 & 0 & 1 & 0 \end{pmatrix}, \quad (\text{B1})$$

$$T_1^- = \begin{pmatrix} 0 & 1 & 0 & 0 \\ -1 & 0 & 0 & 0 \\ 0 & 0 & 0 & -1 \\ 0 & 0 & 1 & 0 \end{pmatrix}, \quad (\text{B2})$$

$$T_2^+ = \begin{pmatrix} 0 & 0 & 0 & 1 \\ 0 & 0 & 1 & 0 \\ 0 & 1 & 0 & 0 \\ 1 & 0 & 0 & 0 \end{pmatrix}, \quad (\text{B3})$$

$$T_2^- = \begin{pmatrix} 0 & 0 & 0 & 1 \\ 0 & 0 & 1 & 0 \\ 0 & -1 & 0 & 0 \\ -1 & 0 & 0 & 0 \end{pmatrix}, \quad (\text{B4})$$

$$\bar{\sigma} = \begin{pmatrix} \sigma_1(\vec{x}) & 0 & 0 & 0 \\ 0 & \sigma_2(\vec{x}) & 0 & 0 \\ 0 & 0 & \sigma_3(\vec{x}) & 0 \\ 0 & 0 & 0 & \sigma_4(\vec{x}) \end{pmatrix}. \quad (\text{B5})$$

and the $\bar{\sigma}$ matrix is

*Present address: Theoretische Physik, University of Wuppertal, 5600-Wuppertal 1, Germany.

¹K. G. Wilson, Phys. Rev. D **14**, 2445 (1974).

²M. Creutz, L. Jacobs, and C. Rebbi, Phys. Rep. **95**, 201 (1983).

³J. B. Kogut, Rev. Mod. Phys. **55**, 775 (1983).

⁴*Lattice Gauge Theories and Monte Carlo Simulations*, edited by C. Rebbi (World Scientific, Singapore, 1983).

⁵D. Weingarten, in *Lattice '88*, proceedings of the International Symposium, Batavia, Illinois, 1988, edited by A. S. Kronfeld and P. B. Mackenzie [Nucl. Phys. B (Proc. Suppl.) **9**, 447 (1989)].

⁶G. Batrouni, G. Katz, C. Davies, A. Kronfeld, P. Lepage, P. Rossi, B. Svetitsky, and K. Wilson, Phys. Rev. D **37**, 1589 (1988).

⁷A. Brandt, in *Multigrid Methods*, edited by S. F. McCormick (Dekker, New York, 1988).

⁸J. Goodman and A. D. Sokal, Phys. Rev. D **40**, 2035 (1989).

⁹R. C. Brower, K. J. M. Moriarty, E. Myers, and C. Rebbi, in *Multigrid Methods* (Ref. 7).

¹⁰R. Ben-Av, A. Brandt, and S. Solomon, Nucl. Phys. **B329**, 193

(1990).

¹¹G. Mack, in *Nonperturbative Quantum Field Theory*, edited by G. 't Hooft (Plenum, New York, 1988).

¹²J. Kogut and K. G. Wilson, Phys. Rep. **12**, 75 (1974).

¹³K. G. Wilson, in *Recent Developments in Gauge Theories*, proceedings of the Cargèse Summer Institute, Cargèse, France, 1979, edited by G. 't Hooft *et al.*, NATO Advanced Study Institutes Series B: Physics, Vol. 59 (Plenum, New York, 1980).

¹⁴R. H. Swendsen, Phys. Rev. B **20**, 2080 (1979).

¹⁵R. G. Edwards, J. Goodman, and A. D. Sokal, Phys. Rev. Lett. **61**, 1333 (1988).

¹⁶K. H. Mutter and K. Schilling, Nucl. Phys. **B230**, 275 (1984).

¹⁷R. Gupta, S. Güsken, K. H. Mütter, A. Patel, K. Schilling, and R. Sommer, Nucl. Phys. **B314**, 63 (1989).

¹⁸D. J. Thouless, in *Ill-Condensed Matter*, edited by R. Balian (North-Holland, Amsterdam, 1978).

¹⁹V. Vyas, Ph.D. thesis, Boston University, 1990.

²⁰L. P. Kadanoff, Rev. Mod. Phys. **49**, 267 (1977).